Journal of Power Sources 183 (2008) 411–417

Contents lists available at ScienceDirect

Journal of Power Sources

journal homepage: www.elsevier.com/locate/jpowsour

Electrochemical performances in temperature for a C-containing $LiFePO_4$ composite synthesized at high temperature☆

M. Maccario[a], L. Croguennec[a,*], F. Le Cras[b], C. Delmas[a]

[a] CNRS, Université de Bordeaux, ICMCB Site de l'ENSCPB, 87 Avenue Dr A. Schweitzer, 33608 PESSAC Cedex, France
[b] Commissariat à l'Energie Atomique, Laboratoire Composants pour l'Energie DRT/LITEN/DTNM/LCE, 17 rue des Martyrs, 38054 Grenoble Cedex 9, France

ARTICLE INFO

Article history:
Available online 23 May 2008

Keywords:
Lithium-ion batteries
$LiFePO_4$
Electrochemical properties
Cycling in temperature
Structural stability
X-ray diffraction

ABSTRACT

C-$LiFePO_4$ composite was synthesized by mechano-chemical activation using iron and lithium phosphates and also cellulose as carbon precursor; this mixture was heated at 800 °C under argon during a short time. Long-range cyclings at different temperatures (RT, 40 and 60 °C) and at C/20 rate between 2 and 4.5 V vs. Li^+/Li were carried out with this C-$LiFePO_4$ material as positive electrode material in lithium cells. Whatever the cycling conditions used, rather good electrochemical performances were obtained, with a capacity close to the theoretical one and a good cycle life, especially at RT – up to 100 cycles – and at 40 °C with ~80% of the initial capacity maintained after 100 cycles. The electrodes recovered after long-range cyclings were characterized by X-ray diffraction; whatever the cycling temperature no significant structural changes (cell parameters, bond lengths, etc.) were shown to occur. Nevertheless, iron was found to be present at the negative electrode – as already observed by Amine et al. – after long-range cycling at 60 °C: other analyses have to be done to identify the origin of this iron (from an impurity or from $LiFePO_4$ itself) and to quantify this amount vs. that of active C-$LiFePO_4$ material using larger cells.

1. Introduction

The increasing use of lithium-ion batteries in space, automotive and portable applications leads to numerous researches to improve the positive electrode materials already used [1] but also to develop new materials. So, since the work of Padhi et al. [2], olivine-like $LiFePO_4$ appears as an interesting positive electrode material for lithium-ion batteries and has thus been widely studied in the last few years [3–7]. The main issue for $LiFePO_4$ is its low conductivity [6,8]. Optimization of $LiFePO_4$ for good electrochemical performances in lithium-ion batteries has been mainly achieved by synthesizing small particles [9] and by forming an electronic conductive coating, that being often a carbon coating [10–12]. Note that the addition of metallic agents such as Ag and Cu has been also considered to overcome the low electronic conductivity [13]. More recently, Delacourt et al. have synthesized by direct precipitation and pH control a carbon-free $LiFePO_4$ sample with very small particles (140 nm), that shows also optimized electrochemical performances with a good reversible capacity of 145 mAh g^{-1} at C/2 rate [14].

The main goal of our study was at first, as described in Ref. [15], to explore different synthesis conditions, then to characterize the C-$LiFePO_4$ composites synthesized and finally to correlate their physico-chemical and electrochemical properties. Note that whatever the synthesis parameter modified, no significant structural and physico-chemical differences are observed between the C-$LiFePO_4$ composites synthesized, except for small differences – difficult to characterize – from a microstructure point of view (particles and agglomerates size distribution, pore size distribution and nature of carbon coating). Nevertheless, all of these C-$LiFePO_4$ composites show electrochemical properties significantly different from each others, suggesting thus that the microstructure of the materials would be the major key factor to control for optimized electrochemical performances.

Optimized $LiFePO_4$ materials deliver at room temperature reversible capacity close to the theoretical one (*i.e.* 170 mAh g^{-1}) [16,17]. The lithium intercalation/deintercalation reaction occurs as a two-phase reaction between a lithium-rich phase ($Li_{1-\varepsilon}FePO_4$, $\varepsilon \to 0$) and a lithium-deficient phase ($Li_{\varepsilon'}FePO_4$, $\varepsilon \to 0$) at a ~3.45 V voltage vs. Li^+/Li [2,18], two narrow solid–solution domains being observed at the two ends of the electrochemical process [19].

The C-$LiFePO_4$ material, synthesized after a short thermal treatment at 800 °C and called $Fe_{800\text{-fast}}$ in Ref. [20], shows after a few charge/discharge cycles at room temperature promising electrochemical properties (~160 mAh g^{-1} at C/20). The present paper focuses thus on the study of its electrochemical performances, upon

☆ Presented at the IMLB 2006-International Meeting on Lithium Batteries.

* Corresponding author. Tel.: +33 5 4000 2647(2234); fax: +33 5 4000 2761.
E-mail addresses: laurence.croguennec@icmcb-bordeaux.cnrs.fr, crog@icmcb-bordeaux.cnrs.fr (L. Croguennec).

0378-7753/$ – see front matter © 2008 Elsevier B.V. All rights reserved.
doi:10.1016/j.jpowsour.2008.05.045

long-range cycling in laboratory lithium cells at room temperature, 40 or 60 °C. X-ray diffraction and structural Rietveld refinements were also used to check for possible structural changes for $LiFePO_4$ after cycling. Whatever the positive electrode material, and perhaps especially in the case of nanosize materials such as $LiFePO_4$, such a study is indeed interesting in order to get more insight not only in the stability (structural, chemical and surface) of the material upon long-range cycling in classical conditions, but also in aging conditions.

2. Experimental

C-$LiFePO_4$ sample was synthesized as described in Ref. [15] by mechano-chemical activation. The reactants, the iron phosphate, synthesized as already described elsewhere [7], and the lithium phosphate (Aldrich), were mixed such as Li/Fe ∼ 1.05. Cellulose (Aldrich) was also initially added. This 500 mg mixture was ball milled in a planetary mill (Fritsch "Pulverisette 4") using tungsten carbide vessels and agate balls. The resulting mixture was thermal-treated under argon flow in a tubular furnace at 800 °C and the synthesized sample is called Fe_{800} in the following. Note that it is called $Fe_{800\text{-fast}}$ in Ref. [20] to discriminate with that synthesized at 800 °C but with a slow thermal treatment.

Electrochemical tests were done on cast electrodes. These electrodes were obtained from a mixture of 80 wt% C-$LiFePO_4$ active material with 10 wt% carbon conductive additive (Super P, MMM Carbon), 10 wt% polyvinylidene fluoride binder (Solef 6020, Solvay) and 0.8 mg of *N*-methyl pyrrolidone cast on an aluminum foil. This cast foil was dried one night at 55 °C and pellets of 10 mm diameter were punched. These pellets were then pressed at 10 T cm^{-2} and dried 48 h at 80 °C under vacuum. Considering the surface and thickness of these pellets, less than 2 mg of active material were present on each electrode, leading to an estimated error of 5% on the specific capacity. Electrochemical properties of this C-$LiFePO_4$ active material were studied in coin cells containing also a lithium foil as negative electrode, two Celgard® 2400 separators and a Viledon® polypropylene foil wetted by a liquid electrolyte (1 M $LiPF_6$ in a mixture of propylene carbonate (PC), ethylene carbonate (EC) and dimethyl carbonate (DMC) (1:1:3)). These coin cells were assembled in a dry box under argon and cycled in galvanostatic mode at a constant C/20 rate (that corresponds to a theoretical exchange of one electron per formula during charge or discharge in 20 h). Electrochemical tests were carried out either with home-made apparatus or with a Bio-logic VMP1 apparatus. After cycling, the cells were disassembled in a dry box under argon; positive electrodes were rinsed with DMC and dried under vacuum.

Samples for X-ray diffraction (XRD), prepared in the dry box, were maintained in a sample holder which allows to keep a controlled atmosphere around the sample during more than 24 h. XRD data were collected using a PANalitycal X'pert Pro diffractometer (Co Kα radiation, and iron filter, antiscatter slit of 1/2° and divergence slit of 1/4° on the incident beam path). The diffraction patterns were recorded in the [15–75]° (2θ) angular range using a 0.0167° (2θ) step and a constant counting time of 12 s.

For structural studies, XRD patterns were refined by the Rietveld method using the Fullprof program [21]. The peaks profile was described with the Thompson–Cox–Hastings function to take into account the microstructure (size and strains effects) for this material (LaB_6 was used as standard) [21].

3. Results and discussion

As reported elsewhere [15], that C-containing $LiFePO_4$ composite synthesized at 800 °C under argon appears as a pure olivine phase from an XRD point of view. Note that no observation of carbon was possible suggesting, as expected, the formation of a highly divided carbon (very small coherence length) from decomposition of cellulose at 800 °C. The structure of $LiFePO_4$ phase was described in the *Pnma* space group with the cell parameters $a = 10.3294(2)$ Å, $b = 6.0086(1)$ Å, $c = 4.6948(1)$ Å and thus $V = 291.38(1)$ Å^3. As expected from the nominal stoichiometry, the Li/Fe ratio was found from chemical analysis superior than 1 with a "$Li_{1.04}Fe_{0.98}P$" chemical formula and 2.9 wt% of carbon. Furthermore Mössbauer spectroscopy revealed the presence of about 5 at.% of iron(III). Note that the origin of these iron(III) ions is not yet identified. Indeed, combination of neutron and X-ray diffraction, magnetic measurements, has only shown that

(i) The structural model $Li_{1+x}Fe_{1-x}PO_4$ is not valid for $LiFePO_4$ and can thus not explain the Li/Fe ratio larger than 1 and the presence of iron(III) in the sample.
(ii) No ferromagnetic and crystallized containing Fe^{3+}-rich impurities such as Fe_2O_3 and Fe_2P [4,22] are detected in the sample.

Nevertheless, note that in some experimental conditions, a small amount of $Li_9Fe_3(P_2O_7)_3(PO_4)_2$ is observed as impurity. As in the sample concerned by this work the Li/Fe ratio is larger than 1 and ∼5–6 at.% of Fe^{3+} are observed by Mössbauer spectroscopy, we can assume the presence of such a lithium-rich amorphous phase with trivalent iron, especially in synthesis with a very short thermal treatment.

3.1. Long-range electrochemical experiments at different temperatures

Long-range cycling experiments were carried out at various temperatures (RT, 40 and 60 °C) in the [2–4.5] V vs. Li^+/Li voltage window to study for possible changes in the electrochemical behaviour and the structure stability. Fig. 1a gives a comparison of the charge and discharge curves obtained at C/20 rate for the 1st, 20th, 70th and 100th cycles at room temperature. Note that for an easier comparison we have chosen to apply a vertical 0.1 V shift to the charge and discharge curves reported in Fig. 1. Fig. 2 gives capacity change, for an Li || C-$LiFePO_4$ (Fe_{800}) cell charged up to 4.5 V vs. Li^+/Li and discharged down to 2 V vs. Li^+/Li at room temperature. The average reversible capacity obtained in discharge is maintained over the 100 cycles around 160 mAh g^{-1}, that value being close to the theoretical one (∼170 mAh g^{-1}). The shape of the charge and discharge curves shows almost no change even after 100 cycles, in good agreement with the good capacity retention observed upon long-range cycling for Fe_{800} when used as positive electrode in lithium cells. Nevertheless, note that the first cycle is different from the next ones, with higher polarizations at the end of the first charge and discharge, those suggesting that complete lithium deintercalation and intercalation are getting difficult due to limited electronic and/or ionic conductivities. Note also that the difference between the charge and discharge voltage plateau remains small and constant (∼0.10 V) upon long-range cycling and that the irreversible capacity at the end of the first cycle is rather small ($\Delta x \sim 0.05$, *i.e.* ∼9 mAh g^{-1}). Consequently, Fe_{800} exhibits good and stable electrochemical performances upon long-range cycling at room temperature. These results are in rather good agreement with those recently reported by Amine et al. (capacity of 140 mAh g^{-1} at C/3 rate up to 100 cycles) for $LiFePO_4$ materials synthesized by solid-state reaction and coated with ∼3.5 wt% of carbon [23].

Fig. 1b gives a comparison of charge and discharge curves for a Li || C-$LiFePO_4$ (Fe_{800}) cell cycled at 40 °C and at C/20 rate in the 2–4.5 V vs. Li^+/Li voltage window, the corresponding specific capacity change upon 100 cycles is given in Fig. 2. Good capacity retention

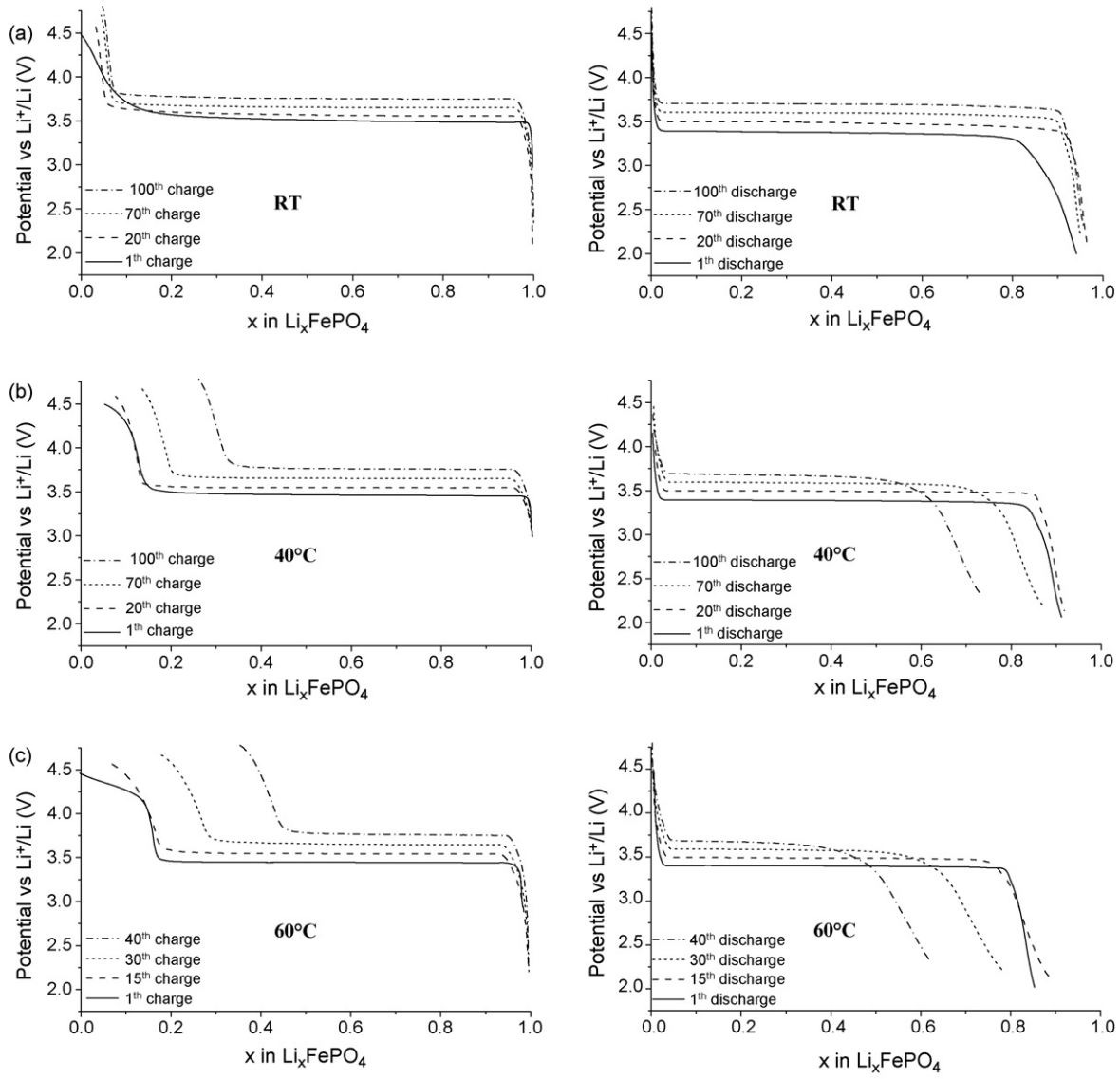

Fig. 1. Cycling curves obtained for Li || C-LiFePO$_4$ (Fe_{800}) cells in the 2–4.5 V vs. Li^+/Li voltage window, at C/20 rate and at RT (a), 40 °C (b) and 60 °C (c). Comparison of the charge curves and discharge curves obtained during the 1st, 20th, 70th and 100th cycles for cyclings at RT and 40 °C and during the 1st, 15th, 30th and 40th cycles for cycling at 60 °C. Each charge/discharge curve is shifted from the previous reported one of 0.1 V for an easier comparison (note that the first charge and discharge are not shifted).

is observed during 50 cycles with an average reversible capacity around 155 mAh g^{-1} (equal within the error on the active mass to that previously reported at RT). As a consequence of increased conductivities at higher temperature, the irreversible capacity and the voltage difference between charge and discharge plateau are slightly smaller than those observed at room temperature. They are equal to ~7 mAh g^{-1} ($\Delta x \sim 0.04$) and to ~0.08 mV, respectively. Considering that the lithium test cells were coin cells made in our lab (*i.e.* in non-optimized conditions), Li || C-LiFePO$_4$ cells with Fe_{800} as positive electrode material show very promising cycling stability even when cycled at 40 °C, indeed more than 80% of the initial reversible capacity is still maintained after 100 cycles. Note that the profile of the first cycle (ends of the 1st charge and discharge) is significantly modified with a temperature increase from RT to 40 °C.

Fig. 1c presents the results obtained for a similar study performed at even higher temperature, *i.e.* at 60 °C. The tendency observed at 40 °C is emphasized at 60 °C, the loss of capacity is faster, about 40% of the capacity is lost after only 40 cycles. The electrochemical characteristics – reversible capacity of ~150 mAh g^{-1} and difference between charge and discharge voltage plateau of ~0.06 mV – observed at the beginning of the electrochemical tests are rather similar to those found at RT and at 40 °C. Note that there is an increase of the irreversible capacity at 60 °C (~25.5 mAh g^{-1} with $\Delta x \sim 0.15$). The comparison of the first charge shape at increasing temperature shows the appearance of a new "plateau" above 4 V vs. Li^+/Li. Nevertheless, the shape of the following first discharge is not strongly affected, only a decrease of the first discharge capacity is observed with an increase of the irreversible capacity; this shows that during the 4–4.5 V vs. Li^+/Li plateau the lithium deintercalation from LiFePO$_4$ is probably still going but together with a secondary process, that is irreversible. This overall phenomenon can be explained if one assumes an irreversible electrochemical reaction occurring on the particle surface (electrolyte oxidation or/and material degradation) whose kinetics increases strongly with temperature. Indeed, this reaction, becoming prevalent when

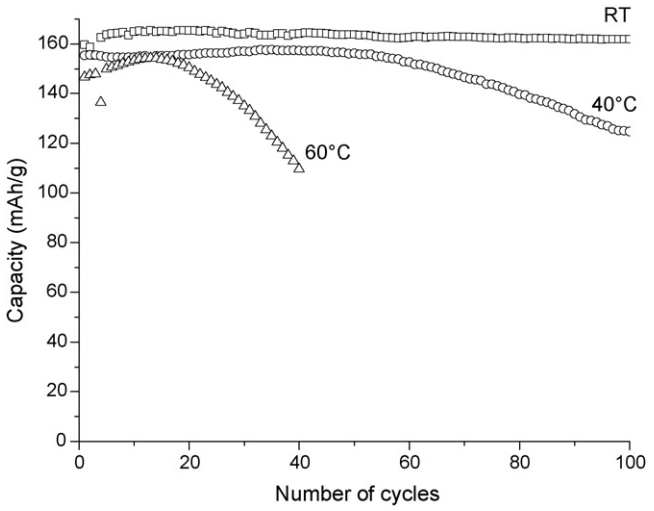

Fig. 2. Evolution of the reversible capacity vs. the number of cycles for Li || C-$LiFePO_4$ (Fe_{800}) cells cycled in the 2–4.5 V vs. Li^+/Li voltage window, at C/20 rate and at RT, 40 °C and 60 °C.

the cell voltage would reach a critical value *i.e.* above 4.13 V vs. Li^+/Li, grows continuously with temperature as shown in the example reported in Fig. 1. Potentiostatic electrochemical tests done at slow scanning rate (10 mV steps every hour) and at room temperature show an increase of an oxidation current (and thus a degradation) from 4.1 V vs. Li^+/Li for the electrolyte used ($LiPF_6$ (1 M), PC:EC:DMC (1:1:3)). We thus assume that the electrochemical reaction occurring at high voltage is associated to the electrolyte degradation, which is promoted by an increase of the cycling temperature in presence of this highly divided C-$LiFePO_4$ material. The greater this electrolyte degradation occurs, the faster the capacity fades. This phenomenon can explain the high irreversible capacity obtained for Li || Fe_{800} cycled at 60 °C, which is indeed partially due to the irreversible capacity associated with the irreversible oxidation of the electrolyte. Moreover, the larger polarization observed at the end of this first charge should decrease with increasing temperature, whereas reverse is effectively observed; thus another effect as electrolyte degradation has to be considered to explain, at least in part, this increase in polarization.

Note that the building of a new coin cell (with fresh electrolyte, separators and lithium negative electrode) using the positive electrode recovered from the cell presented in Fig. 1c leads to the recovering of a discharge capacity around 150 mAh g^{-1}. It reveals that the capacity loss observed upon cycling, at 60 °C for instance, is more probably due to a wetting problem of the positive electrode due to the electrolyte degradation or to a lithium electrode degradation than to the formation of degradation products at the surface of the positive electrode that would lead to increasing resistance.

Using first-principles methods Morgan et al. have recently shown that lithium diffusion occurs through one-dimensional channels along *b*-axis in olivine-type structures and is one order of magnitude faster in $Li_{\varepsilon'}FePO_4$ in comparison to $Li_{1-\varepsilon}FePO_4$ [24]. This result implies significantly different transport properties upon charge and discharge and is in agreement with the observation by Srinivasan and Newman [25,26] of an asymmetric behavior between charge and discharge, *i.e.* a significantly more efficient charge in comparison to discharge in transport limitations conditions. As observed in Fig. 1a, large polarization is observed at the end of the first discharge: in that case it could be well explained by transport limitations because it decreases with an increase in temperature (see Fig. 1b–c).

3.2. X-Ray diffraction study of the materials recovered after long-range cycling

The materials recovered after these experiments, *i.e.* long-range cyclings at room temperature, 40 and 60 °C, were studied from a structural point of view by X-ray diffraction. They are respectively associated to Fe_{800}-RT-100cycles, Fe_{800}-40 °C-100cycles and Fe_{800}-60 °C-40cycles in the following (for instance, Fe_{800}-RT-100cycles corresponds to Fe_{800} cycled at RT during 100 cycles). Fig. 3 compares their X-ray diffraction patterns with those recorded for the pristine material Fe_{800} and for Fe_{800} recovered after a first 1/2 charge (Fe_{800}-RT-1/2charge), after a first charge (Fe_{800}-RT-1charge), after a first charge and a first 1/2 discharge (Fe_{800}-RT-1/2discharge), and finally after one cycle (Fe_{800}-RT-1cycle). Note that these latter materials were obtained upon cycling at C/20 and RT.

The XRD patterns associated to Fe_{800}-RT-1/2charge and to Fe_{800}-RT-1/2discharge are characteristic of a two-phase mixture, as expected from the biphased mechanism observed at ~3.45 V vs. Li^+/Li between the compositions $Li_{1-\varepsilon}FePO_4$ and $Li_{\varepsilon'}FePO_4$. The XRD patterns recorded at the end of the first charge and first discharge are characteristic of single phases, in good agreement with lithium compositions close to $x = 0$ and $x = 1$ for Li_xFePO_4 and belonging thus to the solid–solution domains observed at the very ends of the charge and discharge processes [19]. Fe_{800}-RT-100cycles recovered after a long-range cycling at room temperature shows a XRD pattern characteristic of a single-phase, that being a lithium-rich phase ($Li_{1-\varepsilon}FePO_4$-type), whereas both Fe_{800}-40 °C-100cycles and Fe_{800}-60 °C-40cycles are two-phase mixtures, the main phase being the lithium-rich phase $Li_{1-\varepsilon}FePO_4$ and the other the lithium-deficient phase $Li_{\varepsilon'}FePO_4$. Note that extra-peaks are observed in the 15–22° angular range on the XRD patterns recorded for the electrodes cycled at 40 and 60 °C. They were identified and associated to the Celgard® separator.

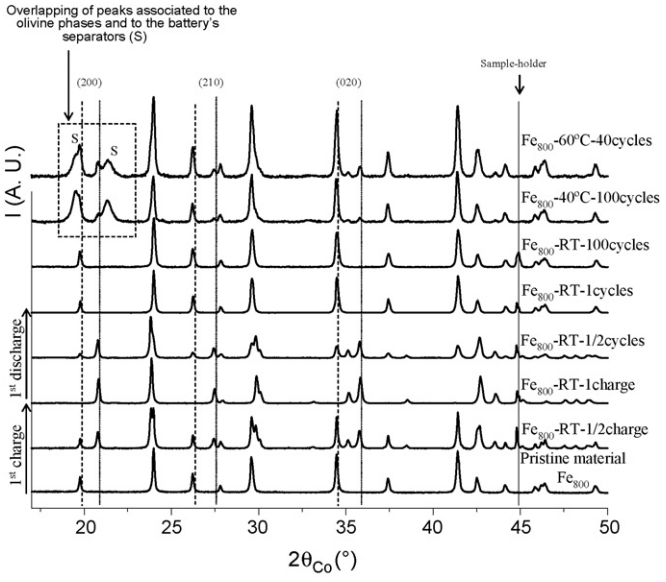

Fig. 3. Comparison of the X-ray diffraction patterns recorded for the pristine material Fe_{800}, Fe_{800} after 1/2 charge at C/20 and at room temperature (Fe_{800}-RT-1/2charge), Fe_{800} after a first charge at C/20 and at room temperature (Fe_{800}-RT-1charge), Fe_{800} after a first charge and 1/2 first discharge at C/20 and at room temperature (Fe_{800}-RT-1/2discharge), Fe_{800} at the end of a first electrochemical cycle at C/20 and at room temperature (Fe_{800}-RT-1cycle), Fe_{800} after 100 cycles at C/20 rate and at room temperature (Fe_{800}-RT-100cycles), Fe_{800} after 100 cycles at C/20 rate and at 40 °C (Fe_{800}-40 °C-100cycles) and Fe_{800} after 40 cycles at C/20 rate and at 60 °C (Fe_{800}-60 °C-40cycles).

In order to determine accurately the structure of Fe_{800}-RT-100cycles and to identify possible changes vs. that of the pristine material Fe_{800}, refinement by the Rietveld method of the XRD data was performed using the Fullprof program [21]. Firstly, a full pattern matching refinement allowed to determine the lattice parameters – the unit cell was described in the *Pnma* orthorhombic space group with $a = 10.3224(5)$ Å, $b = 6.0025(3)$ Å and $c = 4.6988(3)$ Å – and the profile parameters of the pseudo-Voigt function used to describe the shape of the diffraction lines. Then, the structural refinement was carried out by considering the $[Li]_{4a}[Fe]_{4c}PO_4$ structural hypothesis. The Li/Fe ratio being very close to 1, it was thus fixed to 1. The isotropic atomic displacement parameters (Biso(Å^2)) were refined. All the structural and profile parameters obtained by the refinement by the Rietveld method of the XRD data recorded for Fe_{800}-RT-100cycles are given in Table 1, whereas Fig. 4 gives a comparison of the experimental and calculated XRD patterns. The small reliability factors ($R_{wp} = 12.8\%$ and $R_B = 5.57\%$) and the rather good minimization of the difference $|I_{obs} - I_{calc}|$ function suggests a good description of the structure of Fe_{800}-RT-100cycles by the structure of the lithium-rich olivine-type phase. The main structural parameters determined for the Fe_{800} and Fe_{800}-RT-1cycle materials are summarized in Table 2 for comparison. The cell parameters and the cell volume ($V = 290.52(3)$ Å^3 for Fe_{800}-RT-100cycles) are slightly smaller than those determined for the pristine material Fe_{800} ($V = 291.38(1)$ Å^3) and for Fe_{800}-RT-1cycle ($V = 290.95(4)$ Å^3) (Table 2), the cell volume decrease being associated to a decreasing lithium amount in the solid–solution phase $Li_{1-\varepsilon}FePO_4$, as expected after an increasing number of cycles. Comparison of average bonds of Fe_{800}-RT-100cycles (P–O ~ 1.54 Å, Fe–O ~ 2.16 Å, Li–O ~ 2.15 Å) with Fe_{800} (P–O ~ 1.54 Å, Fe–O ~ 2.17 Å, Li–O ~ 2.14 Å) shows no significant change.

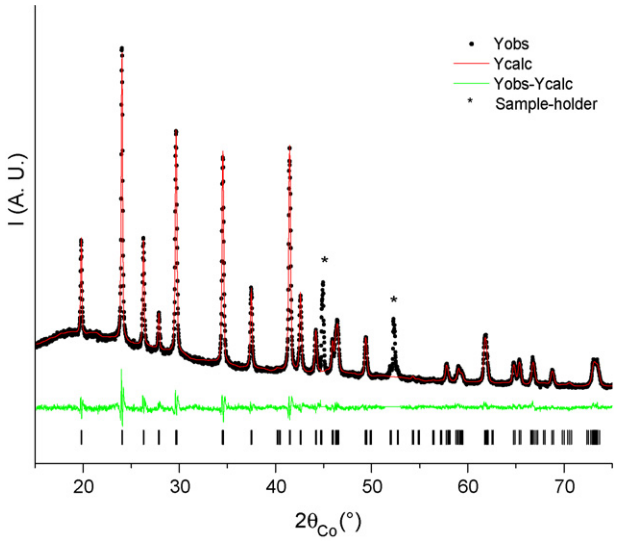

Fig. 4. Comparison of the experimental and calculated X-ray diffraction patterns of Fe_{800} recovered after 100 cycles of an Li || C-$LiFePO_4$ (Fe_{800}) cell between 2 and 4.5 V vs. Li^+/Li, at a C/20 rate and at RT (Fe_{800}-RT-100cycles).

For Fe800-RT-100cycles, structural study shows that there is no significant structural change of Fe800 after 100 cycles between 2 and 4.5 V vs. Li+/Li at C/20 rate and at room temperature.

Table 1
Structural and profile parameters obtained by the Rietveld refinement of the X-ray diffraction pattern recorded for Fe_{800} after 100 cycles at C/20 and at room temperature (Fe_{800}-RT-100cycles)

Fe_{800}-RT-100cycles						
Space group: *Pnma*						
$a = 10.3224(5)$ Å						
$b = 6.0025(3)$ Å						
$c = 4.6888(3)$ Å						
$V = 290.52(3)$ Å^3						
	Site	Wyckoff positions			Occupancy	B (Å^2)
Li	4a	0	0	0	1	4 (2)
Fe	4c	0.2823 (6)	1/4	0.976 (2)	1	4.6 (3)
P	4c	0.095 (1)	1/4	0.416 (3)	1	3.4 (3)
O_1	4c	0.097 (3)	1/4	0.740 (6)	1	4.4 (9)
O_2	4c	0.460 (3)	1/4	0.201 (3)	1	2.9 (7)
O_3	8d	0.165 (2)	0.041 (3)	0.289 (3)	1	2.8 (5)
Conditions of the run						
Temperature						300 K
Angular range						$15^\circ \leq 2\theta \leq 75^\circ$
Number of points						3584
Displacement sample holder (2θ)						$-0.171(3)^\circ$
Number of fitted parameters						24
Profile parameters						
Thompson–Cox–Hastings function						
$Y = 0.088(4)$						
$U = 0.12(1)$						
$V = -0.0017$ fixed[a]						
$W = 0.00383$ fixed[a]						
Conventional Rietveld R-factors for points with Bragg contribution						
$R_{wp} = 12.8\%$; $R_B = 5.57\%$						

Note: Standard deviations have been multiplied by 3, the Scor parameter being 2.75.
[a] LaB_6 used as standard.

Table 2
Comparison of the cell parameters obtained by the Rietveld refinement of the X-ray diffraction patterns recorded for the pristine material Fe_{800}, Fe_{800} after 1/2 charge at C/20 and at room temperature (Fe_{800}-RT-1/2charge), Fe_{800} after a first charge at C/20 and at room temperature (Fe_{800}-RT-1charge), Fe_{800} after a first charge and a 1/2 first discharge at C/20 and at room temperature (Fe_{800}-RT-1/2discharge), Fe_{800} at the end of a first electrochemical cycle at C/20 and at room temperature (Fe_{800}-RT-1cycle), Fe_{800} after 100 cycles at C/20 rate and at room temperature (Fe_{800}-RT-100cycles), Fe_{800} after 100 cycles at C/20 rate and at 40 °C (Fe_{800}-40 °C-100cycles) and Fe_{800} after 40 cycles at C/20 rate and at 60 °C (Fe_{800}-60 °C-40cycles)

	a (Å)	*b* (Å)	*c* (Å)	*V* (Å^3)
Fe_{800}-60 °C-40cycles	10.3263(6) 9.821(2)	6.0057(4) 5.7917(9)	4.6931(4) 4.7852(8)	291.05(4) 272.17(9)
Fe_{800}-40 °C-100cycles	10.3236(6) 9.822(8)	6.0042(4) 5.790(1)	4.6926(4) 4.782(2)	290.87(3) 271.9(3)
Fe_{800}-RT-100cycles	10.3224(5)	6.0025(3)	4.6888(3)	290.52(3)
Fe_{800}-RT-1cycle	10.3239(6)	6.0050(4)	4.6932(4)	290.95(4)
Fe_{800}-RT-1/2discharge	10.314(1) 9.820(1)	6.0011(8) 5.7921(5)	4.6941(7) 4.7796(5)	290.55(7) 271.87(5)
Fe_{800}-RT-1charge	9.8207(8)	5.7913(4)	4.7798(5)	271.85(4)
Fe_{800}-RT-1/2charge	10.3224(6) 9.828(1)	6.0043(4) 5.7955(4)	4.6932(4) 4.7815(4)	290.88(4) 272.32(4)
Fe_{800} (pristine material)	10.3294(3)	6.0086(2)	4.6948(1)	291.38(1)

The electrode material recovered after long-range cycling at 40 °C was also characterized from a structural point of view using X-ray diffraction. A very similar Rietveld refinement – to that described just previously – was performed to analyze the Fe_{800}-40 °C-100cycles X-ray diffraction data, except that two phases were taken into account. Both phases were described by the olivine-type structure and the structural model $[Li_x]_{4a}[Fe]_{4c}PO_4$, *x* being fixed to 1 and 0 for the lithium-rich $Li_{1-\varepsilon}FePO_4$ and lithium-deficient $Li_{\varepsilon'}FePO_4$ phases, respectively. Fig. 5 gives the comparison of the experimental and calculated X-ray diffraction patterns. A good minimization of the $|I_{obs.} - I_{calc.}|$ difference and rather small reliability factors R_{wp} = 14.4%, $R_{B(Li\text{-}rich)}$ = 5.84% and $R_{B(Li\text{-}deficient)}$ = 11.8% are obtained, showing that this two-phase mixture with olivine-type structures describes well the Fe_{800}-40 °C-100cycles XRD pattern. As shown in Table 2, the cell parameters determined for these two phases are in rather good agreement with those determined for Fe_{800}-RT-1/2discharge that sample being also biphasic and obtained after a partial discharge. Again for Fe_{800}-40 °C-100cycles, there are no modifications of the structure, the bond lengths are very close to those determined for Fe_{800}.

Exactly the same refinement procedure as that used for Fe_{800}-40 °C-100cycles XRD data was followed for Fe_{800}-60 °C-40cycles. A two-phase mixture was also considered. Fig. 5 gives the comparison of the experimental and calculated X-ray diffraction patterns, which shows a really good minimization of the $|I_{obs.} - I_{calc.}|$ difference. As expected from Fig. 6 the reliability factors calculated for the lithiated phase are small R_{wp} = 13.1%, $R_{B(Li\text{-}rich)}$ = 4.27% and $R_{B(Li\text{-}deficient)}$ = 9.86%. Note that all the structural parameters (as reported in Table 2 for instance for the cell parameters) determined for Fe_{800}-60 °C-40cycles are similar to those calculated for Fe_{800}-40 °C-100cycles, showing that no significant structural change occurs upon cycling at high temperature up to 60 °C.

Despite no significant structural change was detected for materials cycled either at RT or at high temperature, we cannot exclude the possibility for iron dissolution upon long-range cycling of C-$LiFePO_4$ composites. Indeed, according to Amine et al. the dissolution of iron into the electrolyte would be due to the iron dissolution from the positive electrode [23]. Nevertheless, Koltypin et al. suggest that iron dissolution occurs only in presence of water or acidic species in the electrolyte due to the formation of HF [27]. Furthermore, results reported recently by Axmann et al. suggest that the iron dissolution would be probably linked to the presence of impurities, indeed they have shown that an Fe_2P content leads to higher iron concentrations in the electrolyte after storage at 60 °C for 2 weeks. This latter study also shows that, despite this

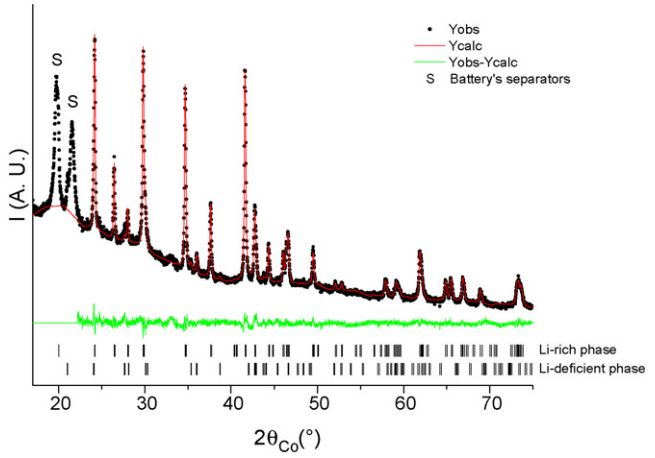

Fig. 5. Comparison of the experimental and calculated X-ray diffraction patterns of Fe_{800} recovered after 100 cycles of an Li || C-$LiFePO_4$ (Fe_{800}) cell between 2 and 4.5 V vs. Li^+/Li, at a C/20 rate and at 40 °C (Fe_{800}-40 °C-100cycles).

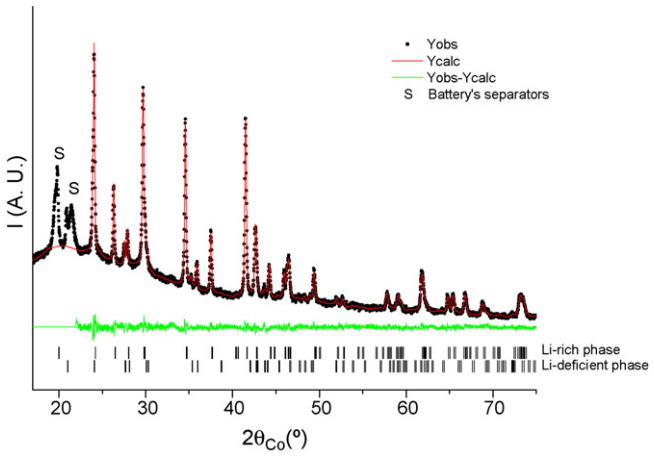

Fig. 6. Comparison of the experimental and calculated X-ray diffraction patterns of Fe_{800} recovered after 40 cycles of an Li || C-$LiFePO_4$ (Fe_{800}) cell between 2 and 4.5 V vs. Li^+/Li, at a C/20 rate and at 60 °C (Fe_{800}-60 °C-40cycles).

iron dissolution problem, $LiFePO_4$ material shows excellent storage stability in electrolyte in comparison with other commercial positive electrode materials such as $LiNi_{1/3}Co_{1/3}Al_{1/3}O_2$, $LiMn_2O_4$, etc. [28].

Note that significant iron dissolution into electrolyte would induce capacity fading and that dissolution would be activated by an increase of the cycling temperature. Indeed, these iron ions, even present as traces, would be reduced at the lithium negative electrode and would then prevent any good reversibility of the redox phenomenon due to the poisoning of the negative electrode and to a decrease of the active electrode mass. In our cycling conditions – in comparison with those used by Amine et al. [23] – slower rate (C/20 vs. C/3), higher temperature (60 °C vs. 55 °C) and higher voltage (4.5 V vs. 4.0 V) should have promoted iron dissolution reactions. At the end of the cycling tests, qualitative analyses by X-ray fluorescence spectroscopy were done on different lithium negative electrodes cycled at 60 °C, it was possible to clearly identify the iron $K\alpha_1$ and $K\beta_1$ peaks on the X-ray fluorescence spectra. Nevertheless, quantitative analyses are necessary for correlating clearly the presence of iron at the negative electrode to a possible capacity fading of C-$LiFePO_4$ composites upon long-range cycling, especially in temperature. Analyses of larger negative electrode recovered from larger cells should allow determining the amount and origin of this iron: from $LiFePO_4$ itself or from an impurity?

4. Conclusions

This study was focused on the electrochemical performances and structural stability of the C-$LiFePO_4$ composite Fe_{800} – synthesized after a short thermal treatment at 800 °C – upon long-range cyclings at different temperatures (RT, 40 and 60 °C) in the 2–4.5 V vs. Li^+/Li voltage window with a C/20 rate.

At room temperature, the Li || C-$LiFePO_4$ (Fe_{800}) lithium cells show small polarization, good reversible capacity ($\sim$160 mAh g^{-1}) and good capacity retention up to 100 cycles. Good capacity retention is also observed during 50 cycles for long-range cyclings at 40 °C, with a good reversible capacity ($\sim$155 mAh g^{-1}, equal within the error on the active mass to that found at RT) and with smaller irreversible capacity and difference between charge and discharge voltage on the plateau than at room temperature, due to the increase of transport properties at higher temperature. After 100 cycles, more than 80% of the initial reversible capacity is still maintained; Li || C-$LiFePO_4$ cells with Fe_{800} as positive electrode material thus show very promising electrochemical performances even when cycled at 40 °C. Long-range cyclings at 60 °C have shown as expected a faster loss of capacity: about 40% of the initial capacity is lost after 40 cycles. Faster degradation of electrochemical performances with the temperature was mainly associated with parasitic reaction above 4.1 V vs. Li^+/Li, as shown by the change in charge profiles – especially the first – at 40 °C and particularly at 60 °C compared with those obtained at room temperature.

Materials recovered after long-range cyclings were studied from a structural point of view by the Rietveld refinement of their X-ray diffraction data. Materials recovered after long-range cycling at RT present a XRD pattern characteristic of a single lithium-rich phase with parameters slightly smaller than those obtained for pristine Fe_{800} and in good agreement with parameters obtained for Fe_{800}-RT-1cycle. Moreover, comparison of P–O, Fe–O and Li–O distances shows no significant structural changes. After long-range cyclings at 40 and 60 °C, a two-phase mixture is obtained with the main phase being the lithium-rich phase $Li_{1-\varepsilon}FePO_4$ and the other the lithium-deficient phase $Li_{\varepsilon'}FePO_4$, the two described with an olivine-type structure. Structural parameters obtained by the Rietveld refinement of their XRD data were shown to be in good agreement with those expected for a $Li_{1-\varepsilon}FePO_4$–$Li_{\varepsilon'}FePO_4$ two-phase mixture.

Note that despite no structural change was detected for Fe_{800}-60 °C-40cycles, qualitative analyses by X-ray fluorescence spectroscopy were done on different lithium negative electrodes after cycling at 60 °C. On the X-ray fluorescence spectra, it was possible to clearly identify peaks due to iron. Nevertheless, quantitative analyses, for example on larger negative electrodes recovered from larger cells, are necessary for correlating clearly the presence of iron (amount and origin) at the negative electrode to a possible capacity fading of C-$LiFePO_4$ composites upon long-range cycling, especially in temperature.

Acknowledgements

the authors wish to thank Cathy Denage (ICMCB) and Carole Bourbon (CEA) for technical assistance, Région Aquitaine (CPER Véhicule Electrique 21-13) and Ademe (PVE no. 0366C0072) for financial support, CEA and CNRS for funding for Magali Maccario (PhD).

References

[1] J.S. Weaving, F. Coowar, D.A. Teagle, J. Cullen, V. Dass, P. Bindin, R. Green, W.J. Macklin, J. Power Sources 97–98 (2001) 733.
[2] A.K. Padhi, K.S. Nanjundaswamy, J.B. Goodenough, J. Electrochem. Soc. 144 (1997) 1188.
[3] A. Yamada, Y. Kudo, K.-Y. Liu, J. Electrochem. Soc. 148 (2001) A747.
[4] P.S. Herle, B. Ellis, N. Coombs, L.F. Nazar, Nat. Mater. 3 (2004) 147–152.
[5] C. Delacourt, P. Poizot, M. Morcrette, J.M. Tarascon, C. Masquelier, Chem. Mater. 16 (2004) 93–99.
[6] A.S. Andersson, B. Kalska, L. Haggstrom, J.O. Thomas, Solid State Ionics 130 (2000) 41–52.
[7] S. Franger, F. Le Cras, C. Bourbon, H. Rouault, Electrochem. Solid State Lett. 5 (2002) A231–A233.
[8] C. Delacourt, J. Rodriguez Carvajal, B. Schmitt, J.M. Tarascon, C. Masquelier, Solid State Sci. 7 (2005) 1506–1516.
[9] G. Arnold, J. Garche, R. Hemmer, S. Strobele, C. Vogler, A. Wohlfahrt Mehrens, J. Power Sources 119 (Special Iss. SI) (2003) 247–251.
[10] H. Huang, S.-C. Yin, L.F. Nazar, Electrochem. Solid State Lett. 4 (2001) A170.
[11] S. Franger, F. Le Cras, C. Bourbon, H. Rouault, J. Power Sources 119 (Special Iss. SI) (2003) 252–257.
[12] S.F. Yang, P.Y. Zavalij, M.S. Whittingham, Electrochem. Commun. 3 (2001) 505–508.
[13] F. Croce, A.D. Epifanio, J. Hassoun, A. Deptula, T. Olczac, B. Scrosati, Electrochem. Solid State Lett. 5 (2002) A47–A50.
[14] C. Delacourt, P. Poizot, S. Levasseur, C. Masquelier, Electrochem. Solid State Lett. 9 (7) (2006) A352–A355.
[15] M. Maccario, L. Croguennec, A. Wattiaux, E. Suard, F. Le Cras, C. Delmas, Solid State Ionics, submitted for publication.
[16] N. Ravet, Y. Chouinard, J.F. Magnan, S. Besner, M. Gauthier, M. Armand, J. Power Sources 97-8 (Special Iss. SI) (2001) 503–507.
[17] S. Franger, C. Bourbon, F. Le Cras, J. Electrochem. Soc. 151 (2004) A1024–A1027.
[18] A.S. Andersson, J.O. Thomas, J. Power Sources 97-8 (Special Iss. SI) (2001) 498–502.
[19] A. Yamada, H. Koizumi, N. Sonoyama, R. Kanno, Electrochem. Solid State Lett. 8 (8) (2005) A409–A413.
[20] M. Maccario, L. Croguennec, F. Weill, F. Le Cras, C. Delmas, Solid State Ionics, submitted for publication.
[21] J. Rodriguez-Carvajal, Laboratoire Léon Brillouin, http://www-llb.cea.fr/fullweb/powder.htm, 2004.
[22] A. Ait Salah, K. Zaghib, A. Mauger, F. Gendron, C.M. Julien, Phys. Stat. Sol. (a) 203 (2006) R1–R3.
[23] K. Amine, J. Liu, I. Belharouak, Electrochem. Commun. 7 (2005) 669–673.
[24] D. Morgan, A. Van der Ven, G. Ceder, Electrochem. Solid State Lett. 7 (2) (2004) A30–A32.
[25] V. Srinivasan, J. Newman, J. Electrochem. Soc. 151 (10) (2004) A1517–A1529.
[26] V. Srinivasan, J. Newman, Electrochem. Solid State Lett. 9 (3) (2006) A110–A114.
[27] M. Koltypin, D. Aurbach, L. Nazar, B. Ellis, in: IMLB, Biarritz, 2006, p. 174.
[28] P. Axmann, C. Stinner, G. Arnold, S. Ströbele, M. Kinyanjui, M. Wohlfahrt-Mehrens, in: IMLB, Biarritz, 2006, p. 176.